Shock Loading of a Cylinder Bank with Imaging and Pressure Measurements

Jason G. Oakley, Mark H. Anderson,
Shaoping Wang, Riccardo Bonazza

July 2001

UWFDM-1160

FUSION TECHNOLOGY INSTITUTE

UNIVERSITY OF WISCONSIN

MADISON WISCONSIN

Shock Loading of a Cylinder Bank with
Imaging and Pressure Measurements

Jason G. Oakley, Mark H. Anderson,
Shaoping Wang, Riccardo Bonazza

Fusion Technology Institute
University of Wisconsin
1500 Engineering Drive
Madison, WI 53706

July 2001

UWFDM-1160

Shock Loading of a Cylinder Bank with Imaging and Pressure Measurements

Jason G. Oakley, Mark H. Anderson, Shaoping Wang, and Riccardo Bonazza

University of Wisconsin–Madison, 1500 Engineering Dr., Madison, WI, 53706, USA

Abstract. Experiments are conducted in a shock tube to study the shock loading of a cylinder and a cylinder bank. The experiments model the loading of the cooling tubes in an inertial confinement fusion reactor where banks of tubes line the reaction chamber. The diffraction of the shock wave is visualized using shadowgraphy. Shock loading of the cylinder(s) is measured with flush mounted piezoelectric pressure transducers located at various angular locations. The single cylinder experiments are compared with the cylinder bank experiments to study the effect of the first wall of cylinders on the second one.

1   Introduction

In proposed inertial confinement fusion (ICF) reactors, a small pellet of fuel is ignited several times a second. This ignition process results in a spherical shock wave radiating into the reaction chamber. In some concept designs, the first structural wall of the reactor is a cooling tube array that absorbs the blast energy and transfers heat to a coolant. Proposed schemes include the Inhibited Flow in Porous Tubes (INPORT) and Perforated Rigid Tube (PERIT) designs [1]. Both designs consist of hollow tubes carrying a PbLi eutectic alloy. The INPORT tubes are made of a porous orthogonal weave of SiC, C, or steel that allows an ablative film of the PbLi to form on the outer surface of the tube. This film absorbs x-rays and target debris. The bulk of the liquid flowing through the tube absorbs the photon and neutron energy and mitigates the isochoric heating by the neutrons. The first few levels of the PERIT design have fan sprays that create a liquid sheet of PbLi between adjacent tubes. This liquid sheet serves the same purpose as the protective liquid film in the INPORT design. These tubes must be able to withstand the impact of the shock wave formed by the thermonuclear reaction of the deuterium-tritium (DT) fuel. Adequately designing the protection for the first wall requires understanding the impulsive shock loading on the tubes. The impulsive loading on the tubes can be understood by studying the interaction of a transient shock wave incident on a cylinder or bank of cylinders. Previous studies include analytical investigations of the shock-refraction phenomenon [2], [3] numerical simulations of the flow around a cylinder [4], [5], [6] and experimental flow visualizations and pressure measurements [7], [8], [9], [10], [11], [12]. These studies provide detailed knowledge of the fluid dynamics around a single cylinder. However, the existing literature contains little work specific to the geometries relevant to the ICF designs.

In an attempt to understand the loading on the first wall of proposed ICF reactors, this work employs a shock tube to study the interaction of incident shocks on a bank of cylinders. Parallel experiments and numerical modeling examine the shock pattern formation and the resulting pressure loading of the cylinders.

2 Experiment

The shock tube is oriented vertically (9.3 m high), has a large square cross-section (25.4 cm) and has a structural capacity of 20 MPa [11]. There are two 22 cm diameter fused silica windows on opposing walls in the test section. Figure 1 shows the layout of the cylinders in the test section. There are two smaller cylinders (radius 2.69 cm) located above a larger, center cylinder (radius 3.175 cm). The size and spacing of the cylinders represent the geometry of the cooling tube arrangement in an ICF reactor. To conduct single cylinder experiments the two smaller cylinders are removed from the test section. There are piezoelectric shock pressure transducers (PCB, model 112A03) mounted flush with the surface of the cylinders as shown in Fig. 2. Four pressure transducers may be mounted to a cylinder in 30° increments. Thus, there are four pressure traces recorded for one upper cylinder and the center cylinder per experiment. Several experiments are conducted with the cylinders mounted to obtain data at 0, 30, 60 and 90 degrees; then the cylinders are rotated 90 degrees to obtain data at 90, 120, 150
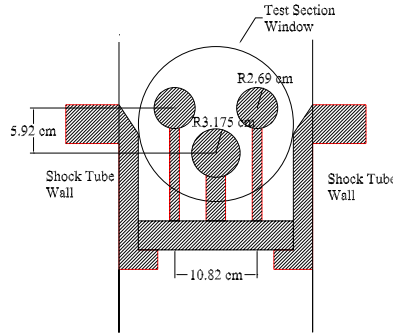
Fig. 1. Side view of cylinder banks detailing the tube size and aspect ratio.
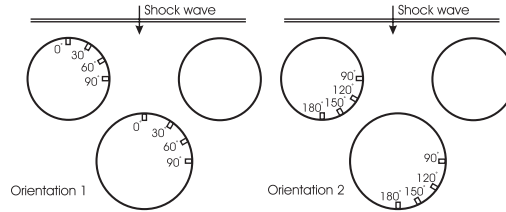
Fig. 2. Cylinder arrangements instrumented with pressure transducers.

and 180 degrees. Therefore, the pressure history around the entire circumference of the cylinder is measured.

Shadowgraphy is used to image the shock diffraction patterns. The light source is one head of a Continuum Surelite II-PIV pulsed Nd:YAG laser. The pulse is 10 ns in duration and can deliver up to 220 mJ/pulse at a wavelength of 532 nm. The central portion of a 0.3 m circle of collimated light is transmitted through the clear size 20.3 cm diameter fused silica windows in the test section. The image is visible on a screen placed on the opposite side of the test section from which the light enters. A Pixel Vision CCD camera (back-lit 1024×1024 pixel array) focused on the screen captures the image. A specified time delay from the shock passing a pressure transducer above the test section synchronizes the laser pulse with the desired position of the shock. One image is obtained per experiment.

Numerical simulations are performed to complement the experiments. The conservative forms of the Euler equations are solved using an exact Riemann solver based Goduov method [12]. A two-dimensional simulation is conducted on a 25.4 cm square domain. The spatial resolution is 0.25 mm. Reflective boundary conditions are chosen for the sides to model the walls of the shock tube. The top of the domain is filled with post-shocked quantities of the gas calculated from one-dimensional gasdynamics. The cylinders are modeled using reflective boundaries on the surface of each cylinder.

3   Results

Experimental results are presented for a M=2.75 shock in argon. A monatomic gas is chosen as it most closely models the low pressure protective Xe blanket used in some reactor designs. Results are presented for both the single cylinder and three cylinders configurations in the form of shadowgraph and schlieren images and force distributions due to the shock loading. Figure 3 shows a shock wave diffracting off of a single cylinder at three different times. The planar shock
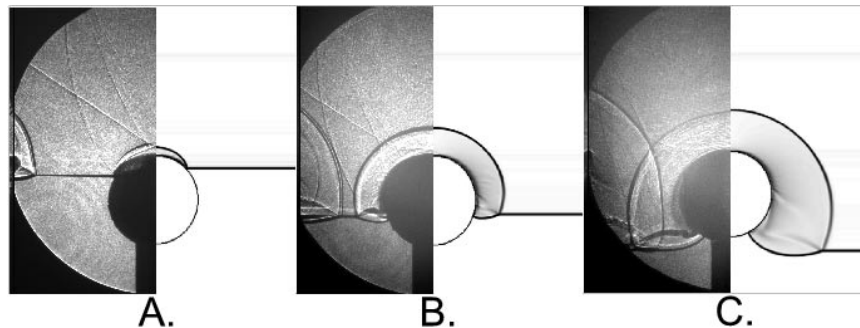
Fig. 3. Comparison between experimental and numerical images for the single cylinder configuration for a M=2.75 shock in argon. The images are for times: A. t=11 μs, B. t=47 μs and C. t=83 μs (from initial contact with the top of the cylinder.)

wave, seen as a flat horizontal line, travels from the top of the imaged region to the bottom. In each of the three images, the experimental shadowgraph image is on the left half while the simulation is on the right. The simulation captures all of the significant features of the experimental image, including: the diffraction of the shock along the cylinder, the reflected shock off of the cylinder and the slip line from the cylinder to the intersection of the incident shock and the reflected shock. In the experimental image, the curved reflected shock on the left is a reflection off of the support structure holding the cylinder.

The shock diffraction patterns for the three cylinder configuration at three different times are shown in Fig. 4. The simulation again seems to capture the relevant features in the experimental image. There is some discrepancy between the experimental and simulation images at t=99 μs, such as the curvature of the reflected shock off of the top of the center cylinder.

A later time simulation image is shown in Fig. 5 to reveal some of the features of the shock diffraction. The following labels are used in the image: IS for the incident shock, RCS for the reflected shock off the upper cylinder(s), RCCS for the reflected shock off of the center cylinder, RWS for the reflected shock off of the wall and CS for the various contact surfaces in the flow field.

The direct measurement of the pressure distribution on the cylinder(s) is indicative of the severity of shock loading. These measurements provide a means for a quantitative comparison with numerical models. When the incident shock contacts the top of the cylinder and subsequently reflects, it imparts a large vertical dynamic load on the cylinder. The magnitude of this load varies with angle along the cylinder, because of the geometry of the shock system. The vertical impulse of a cylinder can be calculated from surface pressure measurements, $P(\theta, t)$:

$$I = \int_0^\tau 2 \int_0^{\theta_m(t)} P(\theta, t)^2 R \cos^2(\theta) L d\theta dt \ . \tag{1}$$

The experimental pressure data is not continuous, but is taken at discrete locations so an approximation to calculate the vertical force as a function of time

A.   B.   C.
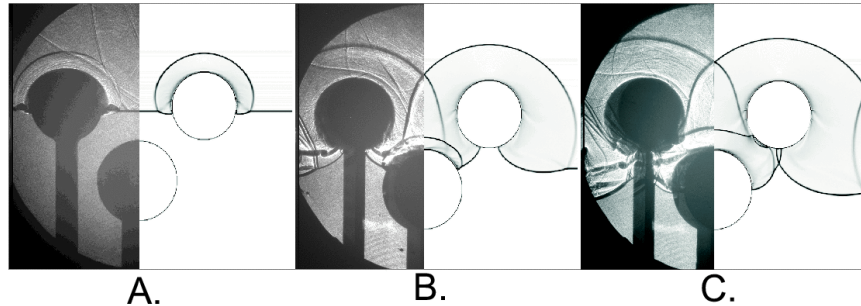
Fig. 4. Comparison between experimental and numerical images for the three cylinder configuration for a M=2.75 shock in argon. The images are for times: A. t=36 μs, B. t=77 μs and C. t=99 μs (from initial contact with the top of the upper cylinder.)

is:

$$F_{vertcal} = 2L[\; A_{0,15} \; (P_{0^\circ} - P_{180^\circ}) + $$
$$A_{15,45} \; (P_{30^\circ} - P_{150^\circ}) + $$
$$A_{45,75} \; (P_{60^\circ} - P_{120^\circ})] \tag{2}$$

where

$$A_{0,15} = R \left[\sin(15^\circ) - \sin(0^\circ)\right],$$
$$A_{15,45} = R \left[\sin(45^\circ) - \sin(15^\circ)\right],$$
$$A_{45,75} = R \left[\sin(75^\circ) - \sin(45^\circ)\right], \tag{3}$$

and the length of the cylinder, L, is 25.4 cm. In order to obtain the vertical force, the pressure at each angular location is multiplied by the projected vertical area of the cylinder surface.

Figures 6 and 7 show force traces for the single cylinder and three cylinders configurations. The maximum force is substantially higher (35%) on the center cylinder in the three cylinder configuration compared with the single cylinder configuration, due to an increase in shock strength as a result of the decreasing area as the shock passes through the first bank of tubes. The dip present in both the data and the numerical model of the upper cylinder is a result of the reflection of the incident shock wave off of the center cylinder, which contacts the bottom of the upper cylinder, substantially decreasing the overall downward vertical force. This is consistent with the time sequence seen in Fig. 4 where at approximately 0.1 ms the reflection is seen to make contact with the upper cylinder. The slight increase in force on the center cylinder at approximately 0.14 ms is the result of a second reflection of the wave off of the bottom of the upper cylinder making contact with the lower. The quantitative agreement between the numerical model and the experimental data are quite good for both the single cylinder and three cylinder configurations.
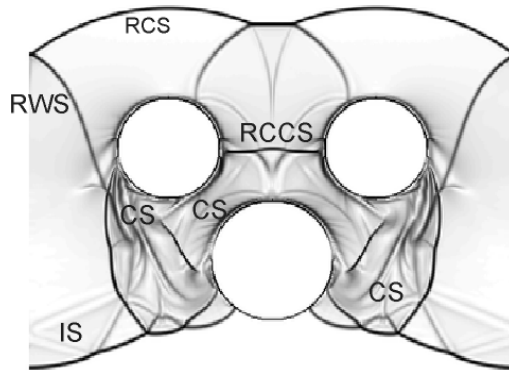
Fig. 5. A late time (144 μs) simulation image obtained with an improved high resolution method (PSM) showing the many shocks and contact surfaces. The mesh size is 0.5 mm.

4   Conclusion

This work attempts to estimate the shock-induced loading on first-wall cooling tubes in proposed ICF reactor designs. Shock tube experiments and accompanying numerical modeling efforts study the interaction between an incident shock wave and cylinder(s) intended to simulate the cooling tubes. The experiments image the shock formations and acquire surface pressure traces. Subsequent calculations from the pressure data yield the vertical force imparted on the cylinders. The model uses an Eulerian code to predict the results from the experiments. Comparisons between experimental and numerical images show good qualitative agreement in the reproduction of the features seen in the experiments. The force data over the cylinder also agrees well and gives a more quantitative comparison between the experiment and numerical model.

References

1. G. Kulcinski, R. Peterson, G. Moses: "Evolution of light ion driver fusion power plants leading to the LIBRA-SP design," Fusion Technology, **26**, pp. 849-856, (1994)
2. T. Bazhenova, L. Gvozdeva, M. Nettleton: "Unsteady interaction of shock waves," Prog. Aerospace Sc., **21**, pp. 249-331, (1984)
3. V. Pavlov: "Diffraction of a strong shock wave on a cylinder with time varying radius," J. App. Mech. Theor. Phys., **26**(6), pp. 806-808, (1995)
4. J. Yang, Y. Liu, H. Lomax: "Computation of shock wave reflection by circular cylinders," AIAA Journal, **25**(5), pp. 683-689, (1987)
5. D. Ofengeim, D. Drikakis: "Simulation of blast wave propagation over a cylinder," Shock Waves, **7**, pp. 305-315, (1997)
6. D. Ofengeim, M. Syshchikova, M. Berezkina, D. Sharov: "Some features of the transient relaxation to a steady-state pressure on the surface of a cylinder acted on by a shock wave," Tech. Phys. Lett., **19**(7), pp. 471-473, (1993)
7. A. Bryson, R. Gross: "Diffraction of strong shocks by cones, cylinders, and spheres," J. Fluid Mech., **10**(1), pp. 1-16 (1961)
8. V. Martin, K. Mead, J. Uppard: "The drag on a circular cylinder in a shock wave," Atomic Weapons Research Establishment Report 0-34/67.
9. V. Bishop, R. Rowe: "The interaction of a long duration shaped blast wave with an infinitely long right circular cylinder," Atomic Weapons Research Establishment Report 0-38/67.
10. J. Oakley, B. Puranik, M. Anderson, R. Peterson, R. Bonazza, R. Weaver, M. Gittings: "An investigation of shock-cylinder interaction," ISSW22 paper 0171, London, UK, pp. 941-946 (1999)
11. M. Anderson, B. Puranik, J. Oakley, P. Brooks, R. Bonazza: "Shock Tube Investigation of Hydrodynamic Issues Related to Inertial Confinement Fusion," Shock Waves, **10**(5), pp. 377-387 (2000)
12. M. Anderson, J. Oakley, M. Coil, R. Bonazza, R. Peterson: "Shock Loading of IFE Reactor Cooling Tubes," 14th ANS Fusion Topical Meeting on the Technology of Fusion Engergy, Park City, UT, USA, Oct 16-19, 2000, **39**(2), pp. 828-833 (2001)
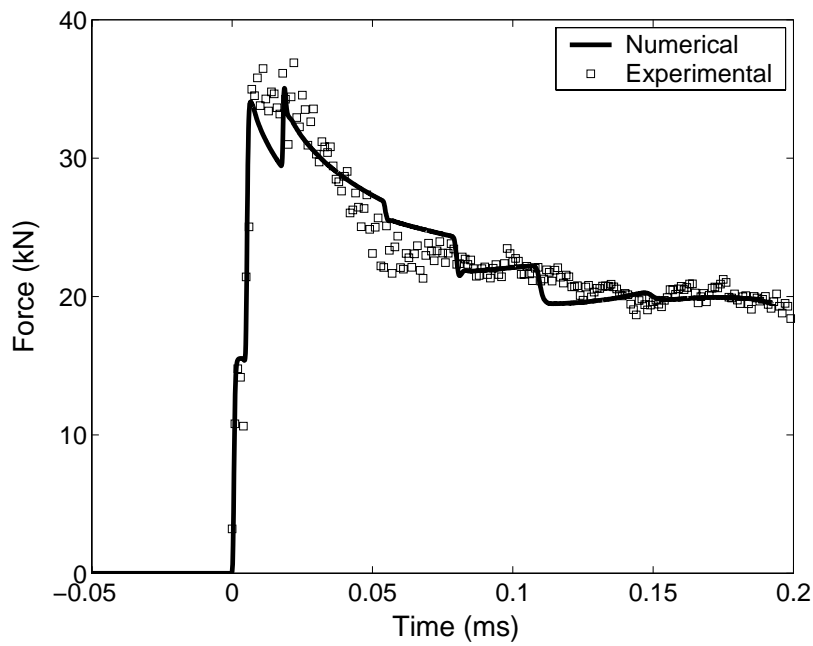
Fig. 6. Force imparted on a cylinder by a M=2.75 shock in Ar. The initial dip in the force (t=0.01 ms) is due to the discrete approximation of Eq. (1) with Eq. (2) (this dip would be eliminated with continuous data and reduced with pressure measurements at more angular locations).
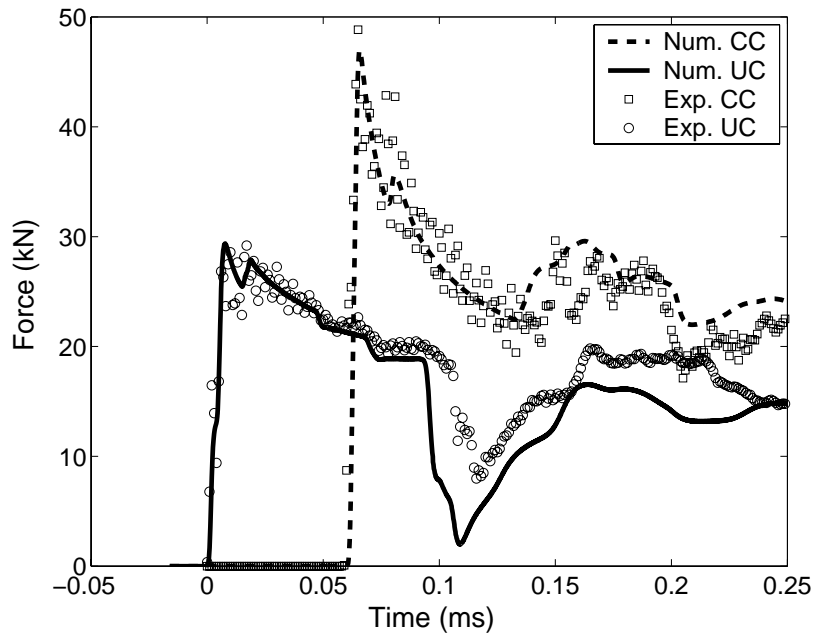
Fig. 7. Force imparted on the upper cylinder(s) and the center cylinder by a M=2.75 shock in Ar.